THESIS

EFFECTS OF GULLY TOPOGRAPHY ON SPACE-TIME PATTERNS OF SOIL MOISTURE IN A SEMIARID GRASSLAND

Submitted by

Joshua J. Melliger

Department of Civil and Environmental Engineering

In partial fulfillment of the requirements

for the Degree of Master of Science

Colorado State University

Fort Collins, Colorado

Summer 2009

COLORADO STATE UNIVERSITY

May 6, 2009

WE HEREBY RECOMMEND THAT THE THESIS PREPARED UNDER OUR SUPERVISION BY JOSHUA J. MELLIGER ENTITLED EFFECTS OF GULLY TOPOGRAPHY ON SPACE-TIME PATTERNS OF SOIL MOISTURE IN A SEMIARID GRASSLAND BE ACCEPTED AS FULFILLING IN PART REQUIREMENTS FOR THE DEGREE OF MASTER OF SCIENCE.

Committee on Graduate Work

Greg Butters, PhD

Brian Bledsoe, PhD

Adviser: Jeff Niemann, PhD

Department Head: Luis Garcia, PhD

ABSTRACT OF THESIS

EFFECTS OF GULLY TOPOGRAPHY ON SPACE-TIME PATTERNS OF SOIL MOISTURE IN A SEMIARID GRASSLAND

Gullies are pervasive topographic features in semiarid grasslands in North America. At the Army's Piñon Canyon Maneuver Site (PCMS) in southeastern Colorado, gullies are important because they restrict the mobility of troops and vehicles in training exercises, and they represent areas that are potentially vulnerable to further erosion. Substantial research has examined the temporal evolution of gullies as well as the factors that initiate gullies and control their morphology. In particular, prolonged periods of low soil moisture (droughts), frequent flash floods, and human activity are thought to reduce vegetative cover and promote gully development. Much less is understood about the feedback of gully topography on space-time patterns of soil moisture. The presence of gullies may produce feedbacks to soil moisture that either enhance or diminish gully development. In this study, field observations from PCMS are used to study the effects of gullies on space-time patterns of soil moisture and to describe the interactions of soil moisture, soil texture, and vegetation around gullies. Three study sites at PCMS have been extensively instrumented. These sites are located in the same broad valley, but one site (~1500 m^2) is ungullied while the other two sites (also ~1500 m^2) each contain a gully. The gully sites are adjacent to each other and their two gullies are approximately parallel. Hourly soil moisture observations have been collected for 8 months at two sites and 4 months at one site using time domain reflectometry (TDR) probes installed along four transects within each site. Each transect contains 6-8 probes that are positioned at the mid-points between topographic breakpoints. Meteorological data are also collected at the ungullied site and between the two gullied sites. Overall, the occurrence of gullies was observed to not affect the spatial average soil moisture within the study sites, but the gullies do promote spatial variability in soil moisture. Gully bottoms tend to be wetter. Although the evidence here is not conclusive, this tendency may be due to gradual lateral inflows, thicker vegetation (which protects the soil against surface crusting and promotes infiltration), and the lower local elevations (which protect against higher wind speeds and evapotranspiration). The gully sidewalls tend to be drier because of rapid drainage during and after precipitation events and in some cases increased solar insolation.

Joshua J. Melliger
Civil and Environmental Engineering Department
Colorado State University
Fort Collins, CO 80523
Summer 2009

ACKNOWLEDGMENTS

The financial support from the U.S. Army Research Office is gratefully acknowledged. Dr. Jeff Niemann provided insight and guidance for this research. We would like to thank Mead Klavetter, Dan Sharps, and Bruce Miller for their logistical support at PCMS. We thank Jonathan Freed, Mike Coleman, and Brandon Lehman for their assistance in the field. We would also like to thank Mike Coleman for his assistance in creating various figures. Finally, we thank Greg Tucker for providing stage data, John Kuzmiak for providing information about available USGS meteorological data, and Jason Ritter from Campbell Scientific Inc. for his technical assistance.

TABLE OF CONTENTS

1. Introduction

Gullying is a significant process in the evolution of landscapes in a variety of climates and soil types, and in many circumstances, it is the main source of sediment at the catchment scale (Patton and Schumm, 1981; Valentin et al., 2005). Gullies are typically defined as small (often ephemeral) channels with steep sidewalls and headcuts that are incising into unconsolidated material (Bradford and Piest, 1980; Schumm et al., 1984) . Gullies pose practical challenges to land managers. From an agricultural perspective, gullies can cause land to be unsuitable for cultivation and/or grazing (Gabris et al., 2003). Gullies are also important issues for managers of military lands. Approximately 70% of Department of Defense lands in the United States are located in semiarid settings (USACE, 1999), where gullies are common features. Gullies can restrict the mobility of troops and vehicles during training exercises, and training exercises involving tracked vehicles can cause degradation of vegetative cover (Doe et al., 1997), which in turn may promote erosion and gully development (Collins and Bras, 2008; Tucker et al., 2006). Military land managers need to mitigate this feedback loop in order to sustainably utilize military lands.

Much research has examined the factors and processes that affect the physical characteristics and evolution of gullies. Tucker et al. (2006) discussed the role that vegetation on the unincised valley floor plays on gully initiation and development. When the vegetation is healthy, erosion thresholds are high, and surface runoff is less likely to erode the underlying material. However, if the vegetative layer has been damaged by phenomena such as a drought, flash flood, fire, or human activity, the land surface is more exposed. Thus, runoff from convective storms is more likely to erode to deeper soil layers where any root density is expected to be lower, causing a positive feedback and increased scour (Tucker et al., 2006).

Spatial and temporal variability of soil moisture is a major factor in the plant regrowth time (Collins et al., 2004; Collins and Bras, 2007; Rodriguez-Iturbe et al., 1999) and therefore plays a significant role in gully formation and expansion. However, spatial and temporal variability of soil moisture was not incorporated into a conceptual vegetation growth and erosion model used by Tucker et al. (2006) because soil moisture has not been extensively monitored for such sites. These authors did observe spatial variation of soil moisture during field inspections, particularly greater wetness in the gully bottoms. Collins and Bras (2007; 2008) recently incorporated spatial and temporal dynamics of soil moisture and vegetation into their landform evolution model to assess their impacts on plant roots and sediment yields. However, the simulated land surfaces consisted of cells with an approximate area of 3600 m^2, which is relatively coarse to describe the variability of elevation, vegetation cover, and soil moisture associated with many gullied systems.

In addition to its role in vegetation regrowth, soil moisture is an integral factor when considering the cohesiveness of a soil and its resistance against erosion processes. For example, soils can lose their strength as water content approaches saturation (Moore et al., 1988). Istanbulluoglu et al. (2005) considered the role of soil cohesion in slab failure, which is a process that significantly affects the shape and evolution of gullies. Gullies that are eroding through soils with low cohesion experience more rapid valley widening by small failures, whereas gullies eroding through high cohesion soils tend to experience fewer but larger failures that result in steeper sidewalls. In a series of model simulations, Istanbulluoglu et al. (2005) focused on describing the physical basis for gully development and assumed no spatial or temporal variability in the model parameters that describe cohesion. However, such variations might occur if the gully topography induces predictable and significant patterns in the soil moisture.

Some field-oriented hydrologic studies have monitored soil moisture variations in and around gully systems. Huo et al. (2008) researched the variability of soil moisture within a 6 m distance perpendicular to gully sidewalls at six locations on a large gully (10 m deep, 28 m wide). The study was conducted in the northern part of the Loess Plateau in China where the climate is semiarid (400 mm annual precipitation). Soil moisture observations were taken at approximately 10 day intervals from July to October, which was a relatively dry period. The authors found that the average soil moisture measured perpendicular to the sidewall face was greater at lower elevations on the sidewall, and soil moisture fluctuations were only observed within 1.5 m perpendicular to the sidewall face. Zheng et al. (2006) studied how soil moisture changes in upland, alfalfa-vegetated areas at various distances from the edge of a gully (the gully was 5-6 m deep and 10-15 m wide). The study was also located in the Loess Plateau, and soil moisture measurements were gathered at unspecified intervals between mid August and mid September at one location and on two dates at two other locations. Zheng et al. (2006) found that average soil water content increased with increasing distance from the gully edge but that sidewall evaporation had little effect on soil moisture at distances of 1.30 m or more.

They also suggested that the effects of evaporation weakened gradually towards the bottom of the gully sidewall.

Other studies have examined soil moisture patterns for cases that are related to but not identical to semiarid gully systems. Fitzjohn et al. (1998) measured surface (0-15 cm depth) soil moisture on a grid with an overall area of 3700 m^2 and a resolution of 5 m within a forested gullied catchment in central Spain (770 mm annual precipitation, 713 mm annual evapotranspiration). This analysis focused on three dates (two in September and one in the following January). Soil texture and vegetation cover at grid points were not measured. It was found that during dry weather conditions, spatial patterns of surface soil moisture were characterized by areas of relatively wet and dry soil, forming a mosaic of sources and sinks for runoff. During wet periods, greater spatial connectivity was observed, resulting in the potential for widespread runoff and erosion. Gomez-Plaza et al. (2001) measured surface soil moisture (0-15 cm depth) across six transects (110-310 m in length, 20 m spacing) each month from December 1996 to April 1998 in semiarid southeast Spain (295 mm annual precipitation, 794 mm annual potential evapotranspiration). Soil texture was measured at each transect sampling location. The transects did not include any gullies, but they did traverse heterogeneous topography that included hillslopes and valleys in a semiarid climate. Because fires burned the vegetation in two out of the three catchments studied, the transects could be classified as vegetated or non-vegetated. Gomez-Plaza et al. (2001) concluded that soil texture, more specifically the negative relationship between percent sand and soil water content, provided the best explanation for spatial variability of soil moisture for burned transects containing low vegetation. In vegetated areas, factors that regulate the presence of vegetation cover such as aspect and profile curvature best explained the spatial distribution of the soil moisture.

Perhaps the most extensive temporal soil water content data in a gully system was collected by van den Elsen et al. (2003) who monitored soil moisture at a 30 min time resolution following rainfall events and a 12 hr resolution during inter-storm periods at a gullied catchment from April 1998 to September 2000 in the Loess Plateau in China (513 mm annual precipitation). Soil moisture at various depths ranging from 15 cm to 154 cm was recorded at 14 locations that focused on different subsystems of the gully—gully floor, sidewalls, and uplands. Only soil moisture data from 1998 was considered for analysis because it was the only year when near average precipitation occurred (five significant rainfall events that produced runoff). The gully sidewalls were on average dryer than the gully floor and upland areas. Van den Elsen et al. (2003) also determined that the greatest soil moisture fluxuations in the gully catchment occurred in upper surface soil layers, but they did not monitor any soil moisture between 0-15 cm depth.

None of the aforementioned studies were able to capture spatial and temporal surface soil moisture patterns in great detail due to the limited number of probes, infrequent sampling times, and/or a limited number of observations at shallow depths. In addition, these studies did not explore the interactions of soil moisture with soil texture and vegetation in gully systems. More data are required in order to bridge this gap and to answer questions such as: What effect does the presence of a gully have on soil texture, and how does soil texture affect surface soil moisture patterns in a gully system? Does the occurrence of a gully have a net effect on site-wide average soil moisture and/or variability? How do gullies affect the spatial distribution of vegetation, and does this variation affect the soil moisture? How does the gully topography affect infiltration during rainfall events and evapotranspiration during inter-storm periods? Answering these questions may lead to enhanced models of gully erosion and the potential impacts of human activities.

The primary objective of this research is to quantify the feedback of gully topography on space-time patterns of soil moisture and to describe the interactions of soil moisture, soil texture, and vegetation around gullies. We begin in Section 2.1 by discussing the location as well as the topographic, soil texture, and vegetation characteristics of three field sites. Section 2.2 describes previously available data for the study sites and gives an overview of the instrumentation installed as part of this study, which includes meteorological and soil moisture monitoring equipment. The soil moisture instrumentation takes measurements at high spatial resolution (~6 m) and temporal frequency (1 hr). Section 3 outlines the key soil moisture observations including the behavior of the spatial average and standard deviation of soil moisture at the three instrumented sites. Each site is also divided into groups based on topographic characteristics, and comparisons between the topographic groups are made. Section 4 interprets the observed variations in soil moisture by analyzing two selected rainfall events using a water budget. This section also discusses how gully topography affects reference evapotranspiration rates by altering solar insolation rates and wind speeds. Finally, Section 5 summarizes the main conclusions.

2. Study Sites

2.1. Site Characteristics

The study area is located within the Burson Arroyo system, a subbasin in the upper reaches of the Taylor Arroyo watershed, at the Army's 987 km^2 Piñon Canyon Maneuver Site (PCMS) in the high plains of southeastern Colorado (Fig 1). The landscape consists of open, gently rolling rangelands interrupted by prominent bedrock scarps (Tucker et al., 2006). Livestock grazing was the primary land use prior to the Army's land acquisition, but it was eliminated after 1983 (Stevens et al., 2008). Since 1985, the land has been periodically used for training by mechanized army units for brigade-sized and smaller maneuvers (Doe and Saghafian, 1992). Streams that drain PCMS are intermittent or ephemeral (von Guerard et al., 1987) and primarily flow into the Purgatory River, a large tributary of the Arkansas River that forms the southern boundary of PCMS. The climate of the study area is semiarid with a mean annual precipitation of ~300 mm and an April through October average evaporation rate of ~1780 mm (von Guerard et al., 1987). Early spring snowstorms can contribute substantial quantities of moisture; however, the majority of precipitation occurs as the result of convective thunderstorms during July through October (von Guerard et al., 1987).

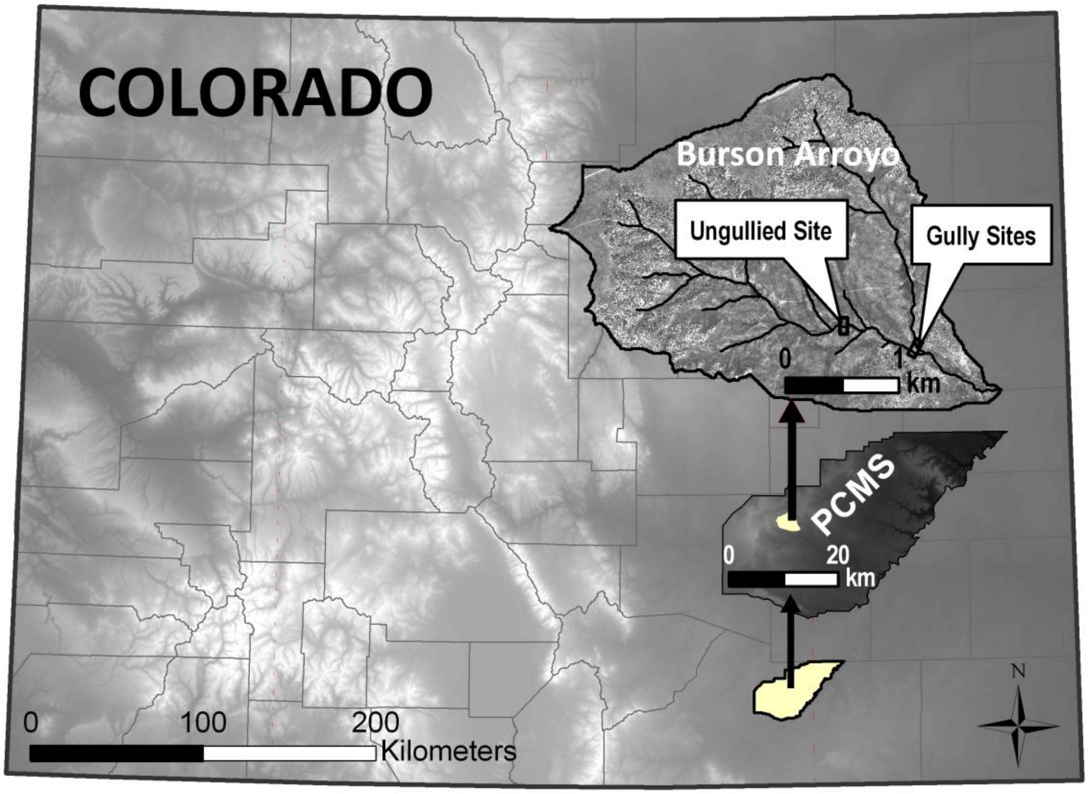

Figure 1. Map of Colorado showing the location of PCMS. Inset shows the topography of PCMS with the location of the Burson Arroyo basin. Second inset shows an aerial photograph of the Burson Arroyo basin with the locations of the ungullied and two adjacent gullied sites.

Three sites, described in this report as the ungullied site, southwest gully site and northeast gully site, were chosen for observation. The sites are all located within the same broad valley and have approximately equivalent areas (~1500 m^2). Topographic surveys were performed at the study sites using a total station and prism. Point elevations from the topographic surveys were interpolated using a spline technique with a tension weight of 0.1 in ArcGIS 9.2 to create a 0.5 m digital elevation model (DEM) and contour map for each site (shown in Fig. 2). These DEMs were then used to calculate site characteristics such as topographic aspect and slope. Aspect was calculated using the ArcGIS spatial analyst toolbox. The ArcGIS toolbox TauDEM (terrain analysis using digital elevation models) developed by David Tarboton of Utah State University was used to calculate slope. Basin characteristics including contributing area were calculated using a United States Geological Survey (USGS) 10 m DEM and tools from Arc Hydro for ArcGIS 9.

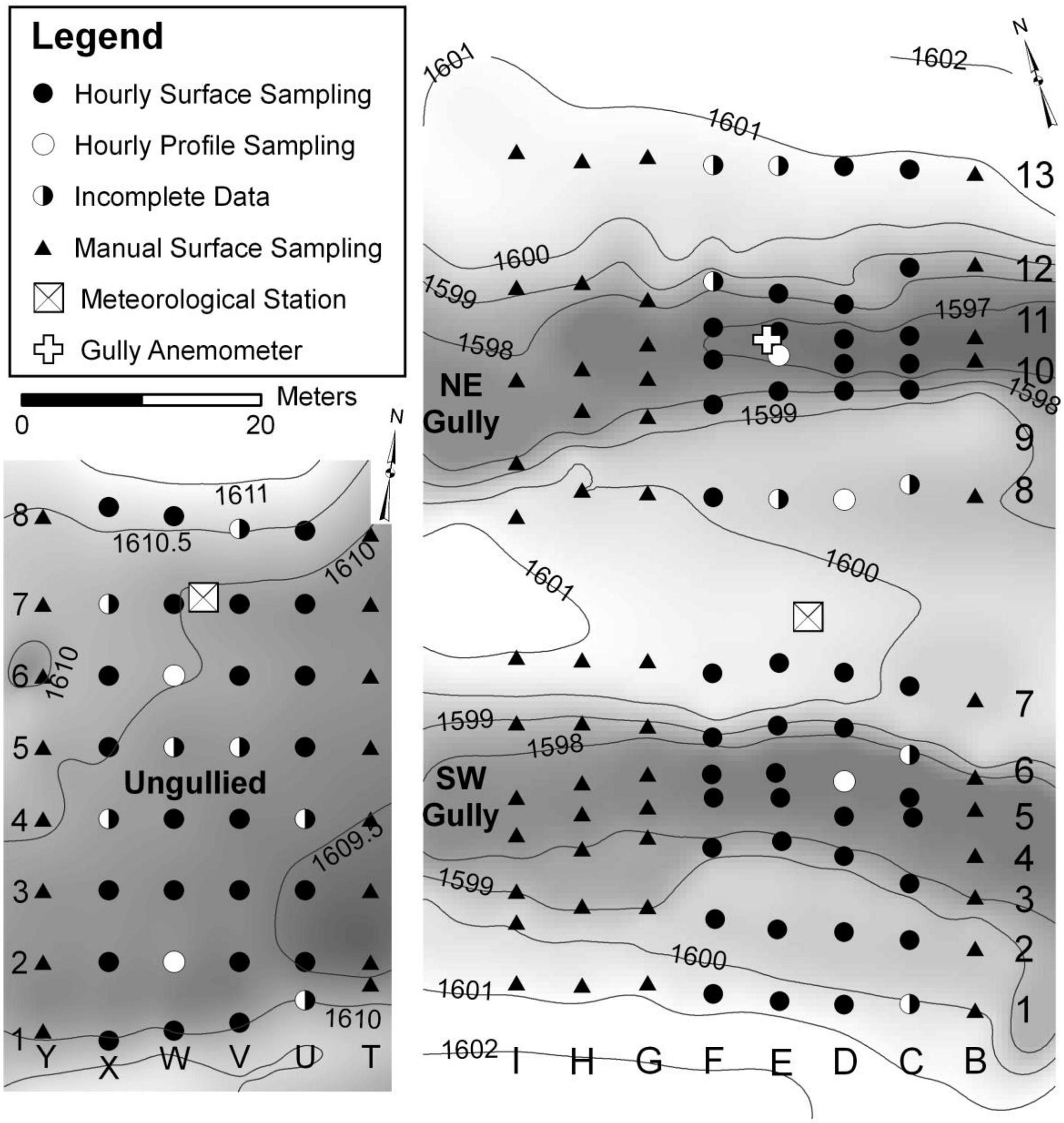

Figure 2. Instrumentation layout at the ungullied site and the two adjacent gullied sites superimposed on a map shaded by elevation (contours provide elevations in meters). Transects are labeled with capital letters, and so-called topographic groups are numbered. Direction of flow in the valley is from left to right in both portions of the figure. North arrows show the orientations of the study sites.

The ungullied site (shown in Fig. 3a) was intended to function as a control group and is located at latitude 37° 29' 35.94" N and longitude 104° 01' 40.20" W. It has a relief of 1 m and consists of an unincised valley that is 40 m in width with mild side slopes. The side slopes may represent the sides of an old gully that has since been refilled to form the current unincised valley floor. The side slopes range from 5-8° on the north-facing slope and 8-13° on the south-facing slope. The upstream contributing area is 3.54 km^2. Within the site, a grid was surveyed that includes 6 transects with 5.5 m spacing (labeled using letters) and 8 points on each transect as shown in Fig. 2. Points along each transect are labeled using numbers. The outermost points on each transect were placed at the midpoints of the side slopes. The inner six points were positioned uniformly with 6 m spacing.

Figure 3. Digital photographs looking upstream at (a) the ungullied site and (b) the two gullied sites. In (b), the southwest gully is on the left, and the northeast gully is on the right. The gully confluence is visible in the foreground. Meteorological stations are visible along the north side slope at the ungullied site and in the upland area between the two gullied sites. Photographs were taken on 7 October 2008.

The southwest gully and northeast gully sites are adjacent to each other (shown in Fig. 3b) at latitude 37° 29' 27.93" N and longitude 104° 01' 13.08" W. The southwest gully is located 700 m downstream of the ungullied site, and the northeast gully site contains a second, approximately parallel gully. The two gullies merge about 50 m downstream from the study sites. Like the ungullied site, the two gullied sites are bounded by side slopes that define a single valley. Except for the occurrence of the gullies, the gullied sites would have relatively low relief. A grid was surveyed across the two gullied sites that includes 8 transects (labeled using letters) and 12-13 points on each transect. As shown in Fig. 2, most points at the gully sites are located at mid-points between breaks in topographic slope; therefore, numbered sets of points are considered as topographic groups because they are located on similar features (e.g., gully bottom or gully sidewall). Physical attributes vary between the gullies. The southwest gully has 6.75 m width and has an average relief of 3 m. Slopes range from 24-30° on the north-facing sidewall and 42-52° on the south-facing sidewall. A terrace is also observed at the southern edge of this study site. The contributing area of the southwest gully is 4.5 km^2. The northeast gully is smaller than the southwest gully. It is 5 m wide and has an average relief of 2.5 m. Sidewall slopes range from 22-47° with the steepest slopes occurring on the north-facing sidewall. The upstream contributing area of the northeast gully is 2.19 km^2. Note that the contributing area of the northeast gully is smaller than that of the ungullied site, and the contributing area of the southwest gully is larger than that of the ungullied site.

The majority of the soil at the study sites is classified as Cadoma clay, characterized by the U.S. Soil Conservation Service (1983) as having low permeability and being at high risk for water erosion. For the present analysis, soil cores approximately 5 cm in diameter and 10 cm in depth were collected for soil texture analysis at all sites on transects T, V, and W (24 locations total) at the ungullied site and transects D, E, and H (38 locations total) at the gullied sites (see Fig. 2 for locations). Percent sand, silt, and clay were measured using the standard hydrometer method and plotted according to the United States Department of Agriculture (USDA) triangle classification using a program developed by Gerakis and Baer (1999). Fig. 4a shows that most locations at the ungullied site are classified as silty clay loam; however, the north side slope (unshaded triangles) is coarser and the south side slope (shaded triangles) is mostly finer than the relatively homogeneous soil of the unincised valley (shaded circles). The majority of the soils at the northeast gully study site (topographic groups 8-13, which are the shaded symbols in Fig. 4b) are silty clay loam and clay loam, which is comparable to the ungullied site. The southwest gully site (topographic groups 1-7, which are the unshaded symbols in Fig. 4b) is typically coarser than the northeast gully and the ungullied sites. Most soils at the southwest gully site are clay loam and loam. Mean percent sand for the soil samples at the southwest gully site is 11.4% greater than the mean percent sand for the northeast gully site. Also in Fig. 4b, shaded circles are a little finer on average than shaded triangles, and unshaded circles are a little finer than unshaded triangles. This observation suggests that within the two gullied study sites, the soils in the uplands and side slopes tend to be a little coarser than the soils in the gully bottoms. However, a clearer division is observed between the points associated with the two gullied sites (i.e. the shaded and unshaded points). Thus, although the local gully topography has a weak influence on the soil texture, the variations between these two adjacent study sites, which are likely unassociated with the modern gullies, are more substantial.

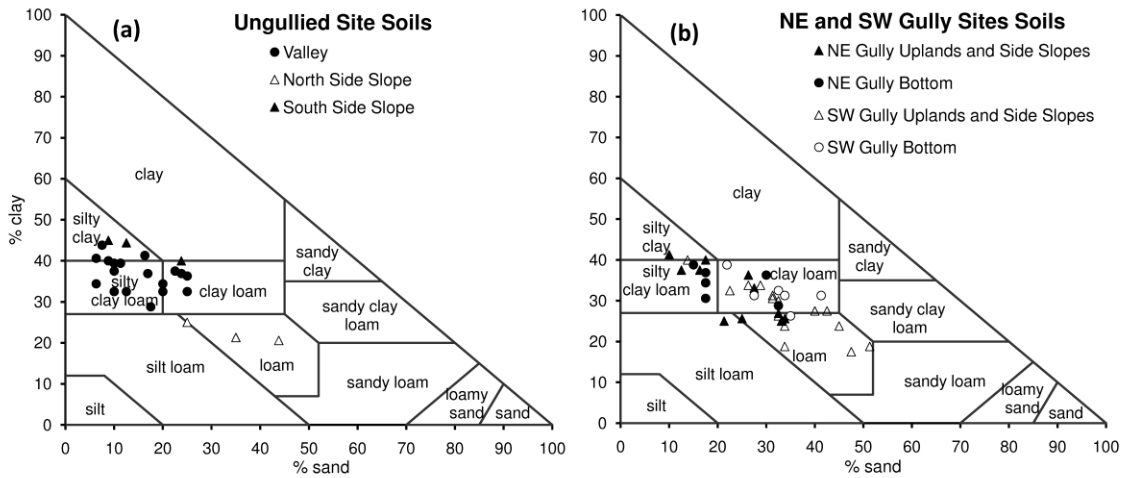

Figure 4. Soil texture results for sampling locations at both the (a) ungullied and (b) southwest and northeast gully sites plotted according to the USDA triangle classification system.

Vegetative cover in the Burson Arroyo system consists primarily of grasslands and open piñon-juniper woodlands (Tucker et al., 2006). The major plant community at the study sites is ATCA/SPAI (Atriplex canescens/Sporobolus airoides), a shrub community including four-wing salt brush and alkali sacation found most commonly along arroyos and intermittent streams (Shaw et al., 1989). In addition to these shrubs, various grasses and cacti are observed at all study sites. Small populations of tamarisk are located upstream and downstream the northeast study site in the gully bottom, and several juniper trees can be found near both gully sites. Visual inspection of the study sites suggest that the thickest vegetation occurs on the ungullied and gully floors while gully sidewalls are often bare (visible in Fig. 3). Valley side slopes and upland areas contain more variable vegetation and are typically less vegetated than gully bottoms. Vegetative cover was measured on 7 and 8 August 2008 at the study sites with a multispectral digital camera (Tetracam Agricultural Digital Camera) from a height of 1.5 m aimed vertically downward. The 3.2 megapixel camera is designed to capture green, red, and near infrared (NIR) wavelengths of reflected light. The digital photographs were analyzed with the image-editing software provided by the camera manufacturer to calculate percent canopy cover in each photograph. The software assists the user in selecting threshold values of red and NIR reflectance that separate live vegetation from soil background and calculates the percentage of the pixels from the selected portion of the photograph that contains live vegetation (Trout et al., 2008). The camera was designed for agricultural use in which green vegetation (high reflectors of NIR light) is easily distinguished from soil. However, much of the vegetation at the study sites was not green when the photos were taken because significant precipitation had not been recorded in over a month. As a result, camera estimates of canopy cover were consistently low relative to visual interpretation of the images (and direct site inspection), but they indicated higher canopy cover where vegetation appeared thicker (e.g., gully bottoms) and lower canopy cover where vegetation appeared thinner (e.g., gully sidewalls). Canopy cover estimates at the ungullied site were not used due to the software's inability to quantify the slight variations in vegetative cover observed at this site when the images were taken. Correlation analysis was performed at the gully sites with percent canopy cover and attributes such as percent sand, percent clay, percent silt, elevation, slope, and aspect. Slope was the only variant that exhibited a statistically significant correlation with percent canopy cover (r^2 of 0.48 and a p value less than 0.01). The regression indicates lower canopy cover on steeper slopes. When only locations with slopes greater than 20° were considered, the r^2 value increased from 0.48 to 0.66, which suggests that the dependence is most important on steep slopes.

2.2. Instrumentation

A significant amount of instrumentation was already available in the vicinity of the sites before the project began. The USGS maintains a network of 12 meteorological stations at PCMS, the closest being approximately 3 km from the study area. Each station measures precipitation, air temperature, relative humidity, wind speed and direction, and soil moisture. In addition, Greg Tucker from the University of Colorado at Boulder maintains three stream gage stations within Burson Arroyo as part of his ongoing research. Each station consists of a siphoning rain gage, an ultrasonic distance sensor with 20 second measurement intervals for 3 hours following most recent bucket tip, and a temperature probe for calculating the speed of sound (used to calculate stage). Two stream gages are located upstream of the adjacent gullied sites, one 280 m upstream of the southwest gully site and the other 110 m upstream of the northeast gully site. The third gage is located 460 m downstream of the confluence of the northeast and southwest gullies.

Newly installed instrumentation includes meteorological stations at the ungullied site and between the two gullied sites (locations shown in Fig. 2). The stations contain a silicon cell pyranometer for measuring incoming shortwave solar radiation in the range of 300-1100 nm, an anemometer mounted 2 m above the soil surface for measuring wind speed, a tipping bucket rain gage with 0.254 mm resolution, two soil temperature sensors for determining periods when the soil reaches the freezing point, and a combined air temperature and relative humidity sensor (ungullied site only). An additional anemometer was installed in the northeast gully bottom to compare wind speeds in the gully and the upland. The instrumentation was programmed to take measurements every 30 seconds and to record hourly averages or sums (as appropriate for each variable). The period of observation of meteorological data is from 06 April 2008 to 30 November 2008 (wind speed and precipitation data at the gully sites are available after 20 April 2008).

Soil volumetric water content was measured hourly using time domain reflectometry (TDR) across transects U, V, W, and X within the ungullied site and transects C, D, E, and F within the southwest and northeast gully sites (locations shown in Fig. 2). Campbell Scientific TDR100's were used at all sites. CS635 probes with three 10 cm tines (modified from 15 cm) were inserted perpendicular to the soil surface to monitor surface soil moisture. Probes were located at the surveyed positions shown in Fig. 2 and remained permanently in position, allowing consecutive measurements at the same location. In addition to monitoring the soil moisture from 0-10 cm depth, soil moisture was measured at depths of 10-20 cm and 20-30 cm at five locations (indicated in Fig. 2 as hourly profile sampling locations). Two of these sites are located at the ungullied site, both in the ungullied valley bottom. Another site is located in the upland separating the two gullies, and the remaining sites are located in each gully bottom. Cables leading from the probes to data loggers were strung through polyethylene split conduit and buried to mitigate rodent damage and minimize effects of temperature on water content values. Additional 10 cm soil moisture readings were taken manually using a portable TDR100 on five dates between 09 March 2008 and 26 June 2008 at the manual sampling locations indicated in Fig. 2, but these are not discussed in this paper for brevity. Similar to the meteorological data, the period of observation for soil moisture at the ungullied and southwest gully sites is 06 April 2008 to 30 November 2008. The period of observation at the northeast gully is only from 07 August 2008 to 30 November 2008 due to equipment problems in the early months. The period of observation ends 30 November because soil temperatures reached the freezing point in December, which affects the reliability of the soil moisture observations.

Volumetric water content was computed internally by the TDR100s using the equation proposed by Topp et al. (1980). The applicability of this equation was evaluated by comparing volumetric water content calculated from 18 undisturbed soil cores with TDR-derived soil moisture at various locations within the study area. Measured water content values ranged from 0.06-0.35 m^3/m^3. Results indicate that mean absolute error for the TDR-derived estimates of soil moisture are 2.1%. However, loose soil surfaces are thought to have caused inconsistencies between the sampling depths of the soil cores and TDR probe sampling depth. In loose soils, 10 cm cores actually include wetter soil from layers deeper than 10 cm because the surface layers consolidate during insertion of the metal core. Removing the four data points where this problem thought to be significant in the field, results in an absolute error of 1.4%.

Hourly data from the installed TDRs were filtered to create a dataset with volumetric water content values at 6 hour intervals (12:00 am, 6:00 am, 12:00 pm, 6:00 pm). When clearly errant values occurred (2% higher or lower than values recorded in the preceding or subsequent hours), values from the preceding and subsequent hours were averaged if those values were judged to be reliable. When obviously errant data were recorded over a series of times, the non-errant value closest in time was used in place of the errant value. If errant data were frequent in the probe's record, that probe was excluded from the analysis. These locations are labeled as “incomplete data” in Fig. 2. Such errant data occurred for a variety of reasons including probe damage and removal by wildlife.

3. Soil Moisture Results

We begin by analyzing how the presence of a gully affects the spatial average soil moisture for each study site and the variability of soil moisture within each study site. Numerous studies have proposed the use of remote-sensing methods to estimate soil moisture patterns (e.g., Idso et al., 1975; Jackson and Schmugge, 1989; Kerr, 2007; Njoku and Entekhabi, 1996; Schmugge, 1983; Wigneron et al., 2003). These methods produce estimates of the spatial average of soil moisture within grid cells that range in size depending on the method. For example, using PCMS as a research location, Nolan et al. (2003) proposed a method that estimates soil moisture at a 50 m grid resolution, but they were unable to verify this method due to difficulties in measuring an equivalent soil moisture value from ground-based measurements. Our instrumented study sites are roughly equivalent to the grid cell resolution used by Nolan et al. (2003).

Site-wide spatial average soil moisture for the ungullied, southwest gully, and northeast gully sites is depicted in Fig. 5a. Precipitation bars show the average total precipitation during six hour intervals from the rain gages at the ungullied site and the upland between the gullied sites (~233 mm total precipitation during the study period). The spatial average soil moisture immediately following precipitation events is similar for all three sites. However, the southwest gully typically drains more quickly following precipitation events and has larger dry-downs than the ungullied and northeast gully sites. The ungullied and northeast gully sites tend to have similar dry-downs. An exception occurs following the early August rainfall events where the ungullied site dries similarly to the southwest gully. This appears to be an anomaly in the behavior of the ungullied site because the behavior of the southwest and northeast gullies remains consistent relative to each other. During the 9-17 August rainfall events, the ungullied site received 5.3 mm less precipitation than the gully sites. Although the peak soil moisture in the top 10 cm of the soil is similar at the ungullied and gully sites following these events as shown in Fig. 5a, the soil moisture measured from 10-30 cm is significantly less at the ungullied site, which suggests that less moisture entered the soil at the ungullied site for this event.

Overall, the differences in the spatial average soil moisture for the study sites are consistent with the differences in soil texture. The ungullied and northeast gully sites have similar textures, and the spatial average for these sites is similar aside from the anomalous event described earlier. This result is interesting because of the significant differences in the topography of these two sites. In particular, there is no clear dependence of the spatial average soil moisture on the presence or absence of a gully. The southwest gully site has coarser soils than the northeast gully site, so it is expected to drain more readily. Fig. 5a confirms this behavior. The spatial-average soil moisture of the southwest gully is on average 13.9% less than that of the northeast gully over the final four months when observations are available at both sites. The fact that both gully sites have comparable topography emphasizes the significance of soil texture on the spatial average soil moisture.

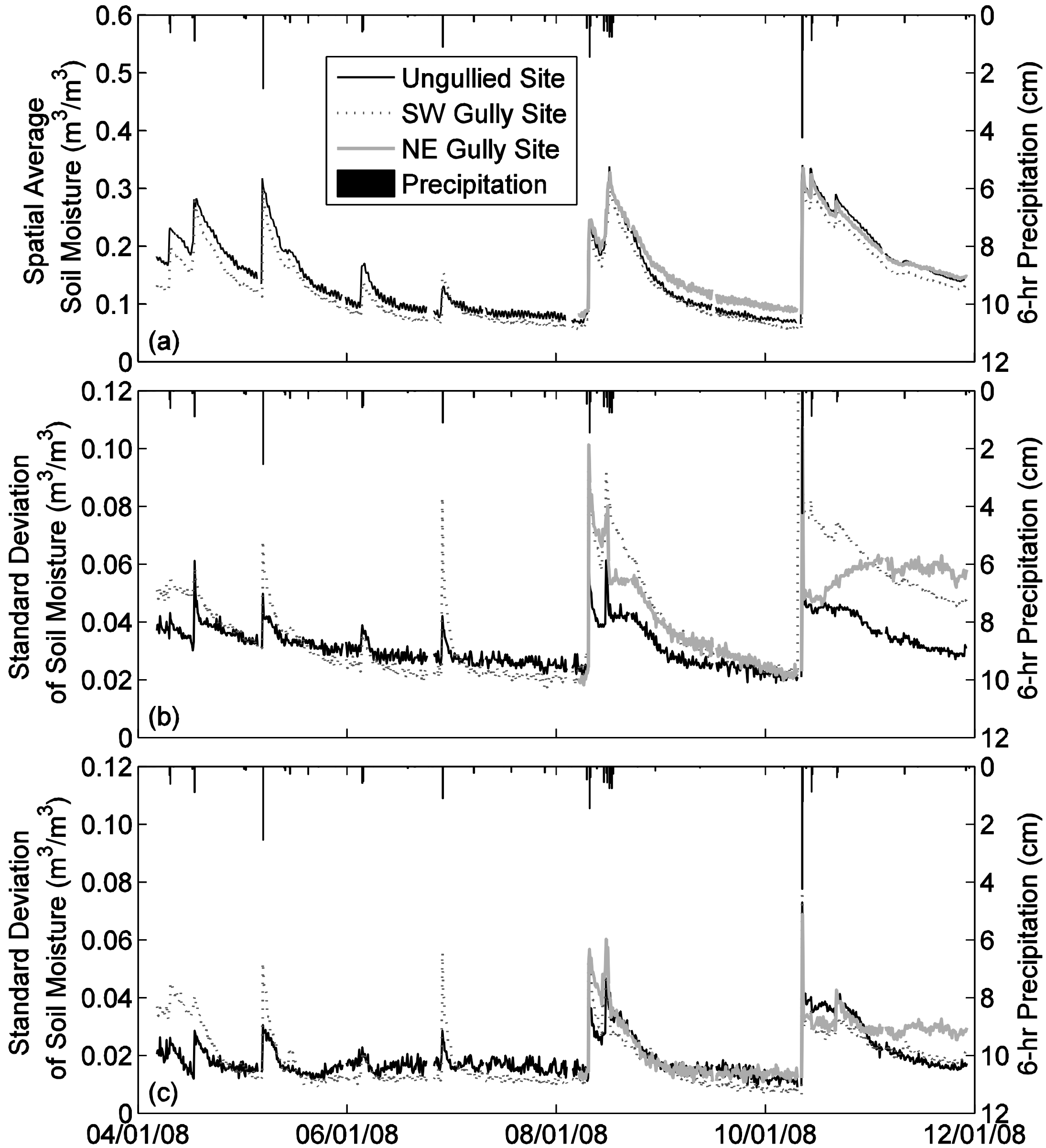

Figure 5. (a) Spatial average soil moisture at the ungullied, southwest gully, and northeast gully sites plotted as a function of time. (b) Standard deviation of soil moisture plotted as a function of time, where the standard deviation was calculated using the values at the individual probes within the three study sites. (c) Standard deviation of soil moisture plotted as a function of time, where the standard deviation was calculated by first averaging the soil moisture within each topographic grouping. Precipitation bars show the average total precipitation during six hour intervals from the rain gages at the ungullied site and the upland between the two gullied sites.

The spatial variability of soil moisture within the three sites is examined next. Fig. 5b shows the standard deviation of soil moisture for each of the three study sites where the standard deviation was calculated using the soil moisture values at the individual probes and the average soil moisture from each study site. Fig. 5c shows the standard deviation of soil moisture for each study site where the standard deviation was calculated by first obtaining the average soil moisture for each topographic grouping and then quantifying the variability of these averages about the site-wide averages. Standard deviation was calculated in this manner to more directly characterize the variability induced by topographic features. The standard deviation in Fig. 5b is typically larger than the value calculated in Fig. 5c. In both cases, the standard deviation is larger at all sites when soil moisture is larger. This is not the case with all other studies of soil moisture variability. Teuling and Troch (2005) show that the dependence of the spatial variability on the spatial average soil moisture differs between sites depending on the relative roles of topography, soils, and vegetation. Comparing between the study sites in Fig. 5c, the standard deviation is typically greater at the gully sites than the ungullied site for the 2-3 days following large precipitation events, possibly suggesting that the gully topography is enhancing the spatial variability. Spatial variability at the gully sites is also higher than the ungullied site during periods with low solar inclination (observed in April and November). During dry periods, the southwest gully is less variable than the ungullied site, which is consistent with its lower spatial average soil moisture. The northeast gully has sustained higher variability during November compared to the ungullied and southwest gully sites. The high variability in this period is the result of unusually large soil moisture at the probes in topographic group 10 in the northeast gully. This area experiences shading due to low sun inclination and the nearby steep north-facing sidewall. Shading is not as significant in the southwest gully due to the nearby terrace and milder sloping sidewall.

To more directly examine the impact of the gully topography on soil moisture, we investigated which topographic groups (i.e. transect points with the same identification number) behave similarly and which behave differently through time. To do this, the spatial average soil moisture for each topographic group was calculated at every time and plotted against the spatial average soil moisture at every time for the other topographic groups. These plots were then analyzed to determine whether a reliable 1:1 relationship occurred. At the ungullied site, the north side slope behaved similarly to the south slope, and the soil moisture at the numbered groups in the unincised valley were comparable. At the gully sites, the upland groups 2 and 7 behaved similarly to the valley side slopes 1 and 13. Also, these upland areas were highly comparable to the ungullied site side slopes. The gully bottoms (4 and 5, 10 and 11) acted relatively similarly to each other except that the northeast gully bottom was consistently wetter than the southwest gully. These gully bottoms behaved similarly to the ungullied valley floor.

For each group of points that was judged to be similar, the spatial average soil moisture was calculated and plotted as a function of time. Looking first at the ungullied site, Fig 6a shows the difference in the behavior of the side slopes (topographic groups 1 and 8) and the valley bottom (groups 2-7). The valley side slopes were consistently drier than the unincised valley bottom during the observation period.

Fig. 6b displays the representative time series for the gully bottom and upland. Because data were not available for the entire observation period at the northeast gully site, representative topographic groups from the southwest gully site were used demonstrate soil moisture differences in the valley slopes and uplands, gully sidewalls, and gully bottoms. During the eight month period, the average soil moisture in the gully bottom at topographic group 5 was 20.1% (0.027 m^3/m^3) greater than the uplands at group 7. Using all data available from 7 August through 30 November, the average soil moisture in the gully bottoms was 17.1% (0.026 m^3/m^3) greater than in the uplands and valley side slopes. This observation contrasts with the results of van den Elsen et al. (2003), who found that soil moisture in uplands was slightly greater than soil moisture in the gully bottoms. In that case, however, the uplands were cultivated, and soil moisture measurements were taken at depths of 15 cm and greater. Here, the field sites are naturally vegetated, and the measurements were taken in the top 0-10 cm of the soil. The wetter conditions in the gully bottoms occur because the gully bottoms exhibit smaller dry-downs than the gully uplands, particularly during June and July, and are persistently wetter during dry periods. Gully bottoms also experience longer peak soil moisture values, probably due to lateral inflow contributions for a period of 7-10 days after sizeable precipitation events. This behavior is most visible in the dry-down at the end of October.

Fig. 6c compares the behavior of the north- and south-facing sidewalls at the southwest gully site with the representative upland group. The gully sidewalls are typically drier than gully bottoms and uplands, which is in agreement with results found by van den Elsen et al. (2003). The sidewalls are drier largely because they do not reach the same high soil moisture values that the uplands attain during storms. They also experience rapid drying following precipitation events. Solar insolation may also produce differences in the dry-down rates of the north- and south-facing sidewalls during periods of low solar inclination (e.g., April and November). During the driest periods, the soil moisture values of the sidewalls become increasingly similar to the soil moisture values of the uplands. In the eight month observation period, the average soil moisture of the gully sidewalls at the southwest gully site was 29.7% (0.047 m^3/m^3) less than the representative gully bottom group (group 5) and 15.6% (0.021 m^3/m^3) less than the representative upland group (group 7). Including both gully sites during the last four months, the average soil moisture of all the sidewalls was 22.1% (0.042 m^3/m^3) less than the gully bottoms and 9.8% (0.015 m^3/m^3) less than the uplands and valley side slopes.

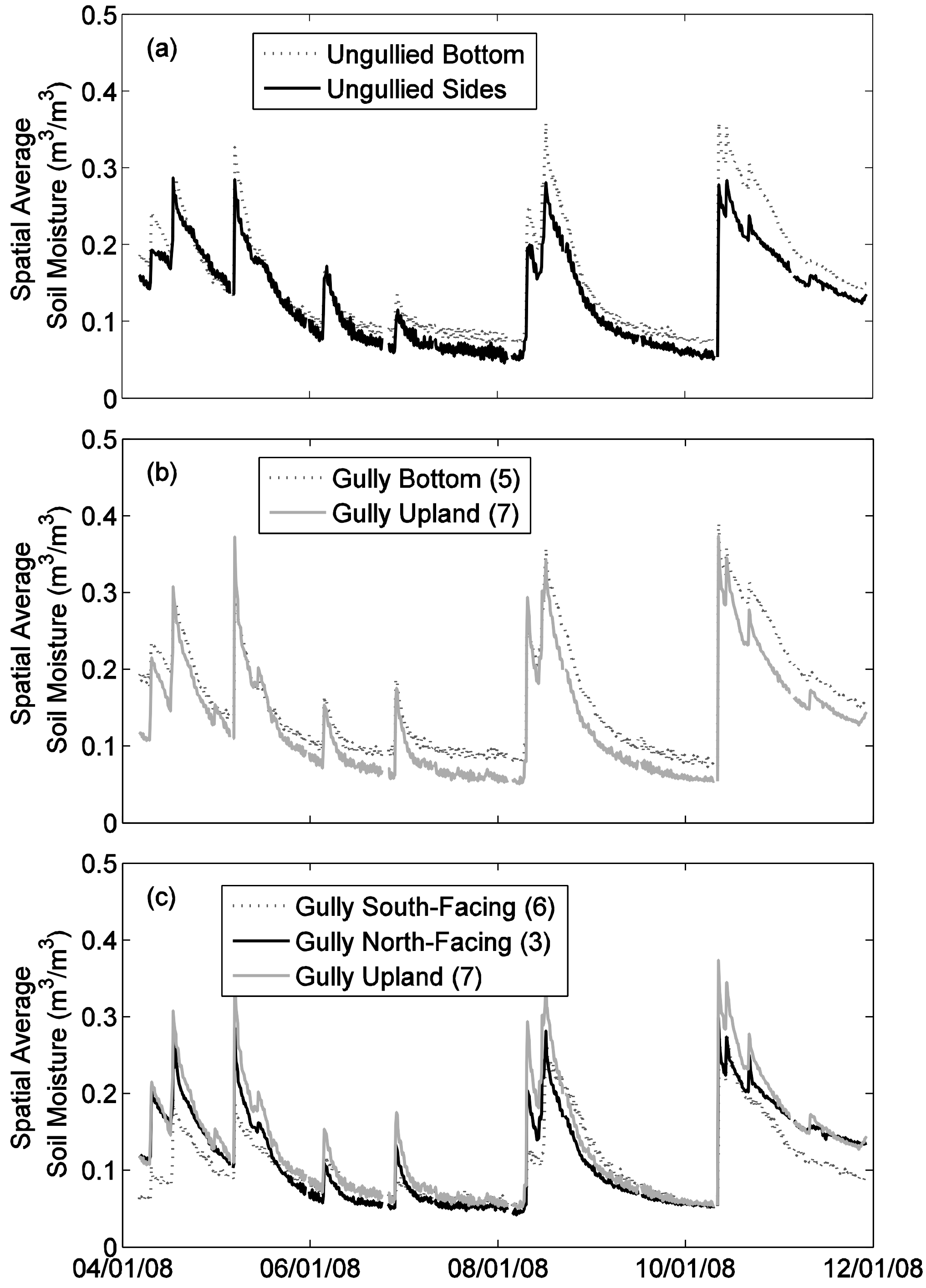

Figure 6. Spatial average soil moisture plotted as a function of time for the (a) ungullied valley bottom and side slope locations, (b) gully bottom and upland locations, (c) upland, north-facing sidewall, and south-facing sidewall locations. The ungullied valley is the spatial average of all probes located between the side slopes. Numbers within parentheses following the legend titles in (b) and (c) indicate the topographic group number chosen to represent the site area.

4. Analysis and Discussion

In order to understand how the gully topography affects soil moisture as observed in Section 3, this section analyzes the topographic influence on the hydrologic processes that determine soil moisture. Changes in surface soil moisture in time can be described in terms of hydrologic processes using a depth-integrated continuity equation,

$$\delta\Delta\theta_1 = P - I - R - E - G + L \tag{1}$$

where δ is the thickness of the soil layer under consideration (10 cm in this case), $\Delta\theta_1$ is the change in the average soil moisture of that soil layer, *P* is the precipitation depth, *I* is the depth of water intercepted by vegetation, *R* is the runoff depth, *E* is the evapotranspiration depth, *G* is the water transferred out the bottom boundary of the soil layer, and *L* is the net lateral inflow to the layer. Note that the water table in the region has been observed to be on the order of tens of meters below the ground surface (von Guerard et al., 1987). During the 8 month observation period, two precipitation events occurred in which the near-surface soil moisture (0-10 cm) responded, but the soil moisture in the deeper layers (e.g., 10-30 cm) exhibited little change (Fig. 7). These events occurred on 10 April and 5 June (encircled in the figure) and both produced ~1 cm of rainfall. Each precipitation event lasted 8 hrs and intensities averaged ~1.3 mm/hr with ranges of 0-2.8 mm/hr during the 10 April event and 0-5.6 mm/hr during the 5 June event. Precipitation data at the gully sites were not available for the 10 April event so comparisons between intensities at the ungullied site and gully sites could not be made; however, rainfall intensities from both gages during the 5 June event were similar.

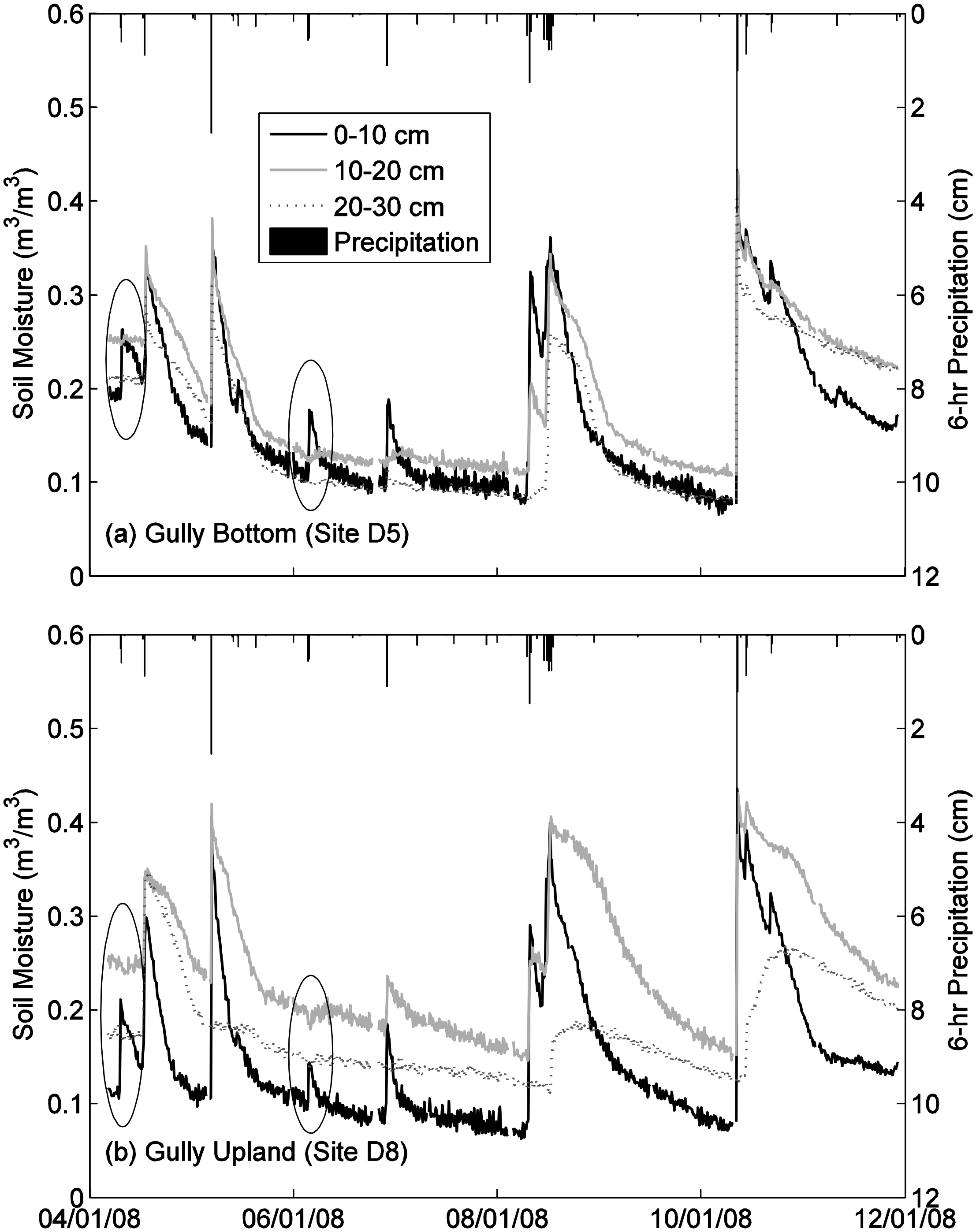

Figure 7. Soil moisture at 0-10 cm, 10-20 cm, and 20-30 cm depths in (a) the gully bottom (probe located at site D5) and (b) the upland (probe located at site D8). The ovals encircle the two precipitation events where the soil moisture below 10 cm does not respond to the precipitation. Precipitation bars give the average total precipitation during six hour intervals calculated from the rain gages at the ungullied site and the gully upland.

Considering the time period from just before each precipitation event to the maximum soil moisture reached after rainfall stops (approximately 10 April 0:00 – 10 April 18:00 and 5 June 6:00 – 6 June 0:00), the soil moisture did not change in the deeper layers, so $G \approx 0$ and:

$$\delta\Delta\theta_1 = P - I - R - E + L\,. \tag{2}$$

During these two events, the stream gages installed by Greg Tucker in the gully bottoms upstream and downstream of the gullied site recorded zero discharge, suggesting no widespread runoff production. However, localized runoff may have still occurred. Lateral flow is also expected to be small at most locations because $G \approx 0$. However, recall that indications of lateral flow were seen in Fig. 6b, so L is retained here for generality. Eq. 2 can be rewritten as:

$$R + I + E - L = P - \delta\Delta\theta_1 \tag{3}$$

where the right side of the equation includes all the measured quantities and the left side collects the unknowns. Positive values of $R+I+E-L$ indicate net losses due to localized runoff, interception, evapotranspiration, or quick (6 hour time period) net lateral outflow (perhaps due to macropores). Negative values indicate net gains from run-on or quick lateral inflow. It should be noted that $\Delta\theta_1$ was calculated by taking the difference of two numbers with error. The result is a small number that may include more substantial error. Thus, we focus on identifying general tendencies from this analysis across the multiple sites, rather than attempting to explain the results at each individual probe.

Fig. 8 shows the calculated $R+I+E-L$ values for the 10 April and 5 June events at each probe location with reliable data at the ungullied and southwest gully sites (because data were available, topographic group 8 from the northeast gully site was included to increase the sample size). Bars represent $R+I+E-L$ for specific locations; triangles indicate the average value for the topographic group. During the 10 April event, the ungullied site experienced an average $R+I+E-L$ of 0.17 cm, which was relatively uniform across the site. The relatively uniform, positive net loss was likely due to the site's relatively homogeneous vegetative cover and its associated interception of rainfall. The southwest gully site had an average $R+I+E-L$ of 0.08 cm for the same event. Consistent net losses are visible in the gully bottom and the steep sidewall, and combinations of losses and gains were observed at other topographic groups. Losses in the gully bottoms were likely caused by greater interception due to the presence of thicker vegetative cover. Losses on the steep gully sidewall are likely due to local runoff and rapid subsurface drainage rather than interception because minimal canopy cover exists at these locations. Any run-on and lateral inflow from the sidewalls into the gully bottom does not overcome the interception losses at these locations. The magnitude of run-on and lateral inflow may be small because the gully bottom probes are located ~1 m from the sidewall toe.

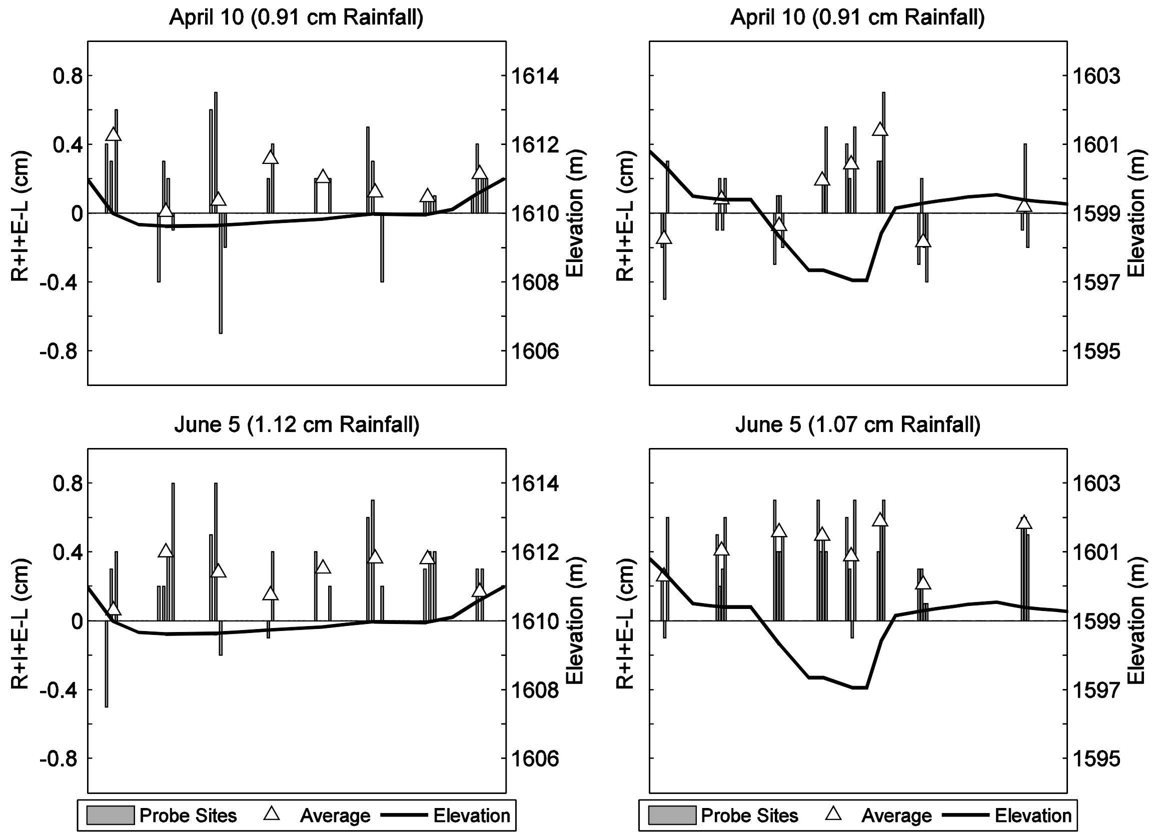

Figure 8. Plots of $R+I+E-L$ for all probe locations with reliable data across the ungullied and southwest gully sites (looking upstream) during the precipitation events identified in Figure 7. Black lines give a representative profile of the sites. Bars represent $R+I+E-L$ for specific locations; triangles indicate the average for the topographic group. Positive values represent net deficits, which suggest importance of runoff, interception, or lateral outflow. Negative values represent net gains, which suggest importance of run-on or lateral inflow.

Fig. 8 shows that the 5 June event produced a similar pattern of net losses at the ungullied site compared with the 10 April event. The average net loss was 0.27 cm for the June event, which is higher than the net loss for the April event. However, much greater losses occurred at the southwest gully (average net loss of 0.42 cm), and net losses were observed at all but two probe locations. Greater losses were possibly caused by higher interception or evapotranspiration associated with thicker vegetative cover at this site during late spring, but because the ungullied site did not experience much increase in $R+I+E-L$, we believe the cause lies elsewhere. One possibility is that surface crusting at this time of year led to reduced infiltration rates. During site visits in early April, we observed that the soil was quite loose in numerous locations, particularly locations with little vegetation. In late May, the soil was noticeably drier and harder with a very compacted crust. Studies have shown that bare soils can develop surface crusts that tend to reduce infiltration rates and promote local runoff and ponding (Bromley et al., 1997; Casenave and Valentin, 1992; Fox et al., 2004; Morin and Benyamini, 1977). More specifically, soil crusts mainly develop on gentle slopes rather than steep slopes (Valentin et al., 2005) where erosion can degrade the surface seal (Poesen, 1986). This may explain why more losses are observed during the June event than the April event at the gullied site, particularly locations with less dense vegetation (the gully valley side slope and uplands). The ungullied site is more homogeneously and thickly vegetated, so it likely did not develop significant surface crusts, explaining the similarity of losses between the two events. The amount of losses observed at the southwest gully during the rainfall event is negatively correlated with percent sand and positively correlated with percent clay during the 10 April and 5 June rainfall events (p values less than 0.05 in all cases except percent clay on 10 April, which was 0.06) as demonstrated in Fig. 9. These correlations agree with past studies that show surface crusting increases with clay content (Agassi et al., 1981; Mills and Fey, 2004; Shainberg and Singer, 1985). It should be noted, however, that the perceived increase in losses at the southwest gully site is based on the assumption that this site received the same precipitation as the ungullied site for the April event when only one rain gage was available (as mentioned earlier).

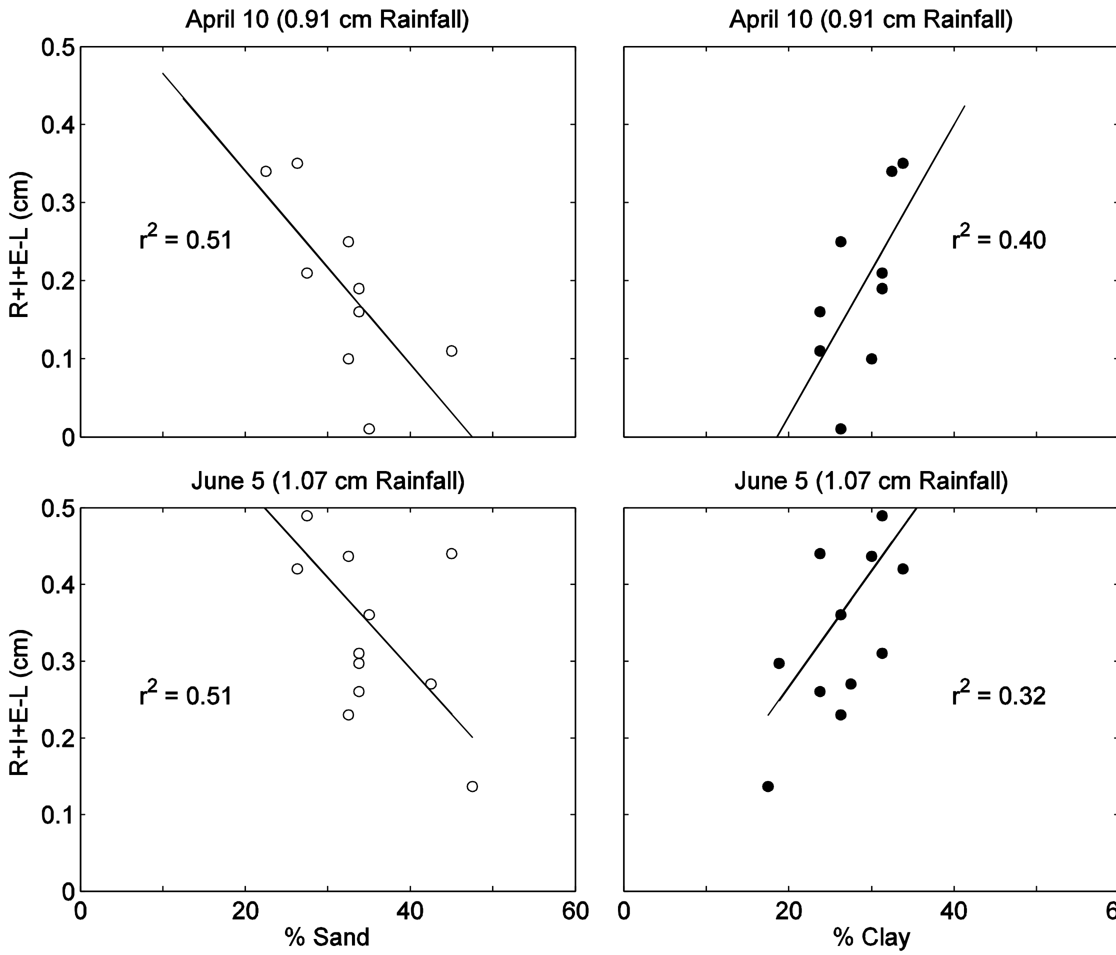

Figure 9. *R+I+E−L* plotted against the % sand and % clay (indicated by the circles) at the southwest gully site for the 10 April and 5 June rainfall events. Linear regressions are shown as black lines.

To further understand the effects of the gullies on the temporal variability of soil moisture, we next examine the behavior between storm events. Specifically, Eq. 1 is applied to the six day period after the two precipitation events described earlier. A six day period was chosen because another rainfall event occurred seven days after the 10 April event. Between rainfall events, $P = 0$, $I = 0$, and $R = 0$. Thus Eq. 1 can be rewritten as:

$$E + G - L = -\delta \Delta \theta_1 . \qquad (4)$$

For the 6 days following the 10 April and 5 June rainfall events, $G \approx 0$ as shown in Fig. 7. Again, lateral flow is expected to be small because $G \approx 0$, but it may occur at some locations shortly after precipitation events. Eq. 4 becomes:

$$E - L \approx -\delta \Delta \theta_1 . \tag{5}$$

This equation simply states that the observed changes in soil moisture in these periods are due to evapotranspiration and the possible net lateral movement moisture.

Fig. 10 depicts the net flux $E - L$ during the six days following the events at each probe location with reliable data. In the figure, bars represent the $E - L$ values for individual probes, and triangles show the average value for each topographic group. Positive values indicate a net loss or outflow of moisture. In comparing the dry-down of each event, the ungullied site typically experiences greater net losses after the 5 June event than the 10 April event, which is expected due to the likelihood of higher reference evapotranspiration rates in June than April. The losses are relatively uniform across the site except for the side slopes following the 10 April event. At the gullied site following both events, the steep gully sidewall experienced less net losses than the other topographic groups. The smaller losses likely occur because the soil moisture at the beginning of the studied time period is smaller than most other locations due to rapid drainage at these steep locations. Likewise, on average the entire gullied site experienced slightly lower net losses following the June event than the April event, corresponding to greater losses during rainfall (possibly due to surface crusting) and the lower peak soil moisture achieved after rainfall. Correlation analysis confirms the association between the initial soil moisture and the loss rate. $E - L$ during the six days following each event is positively correlated with the peak soil moisture achieved after each rainfall event (*p* values less than 0.03), implying that initially wetter soils dry down more quickly than initially drier soils.

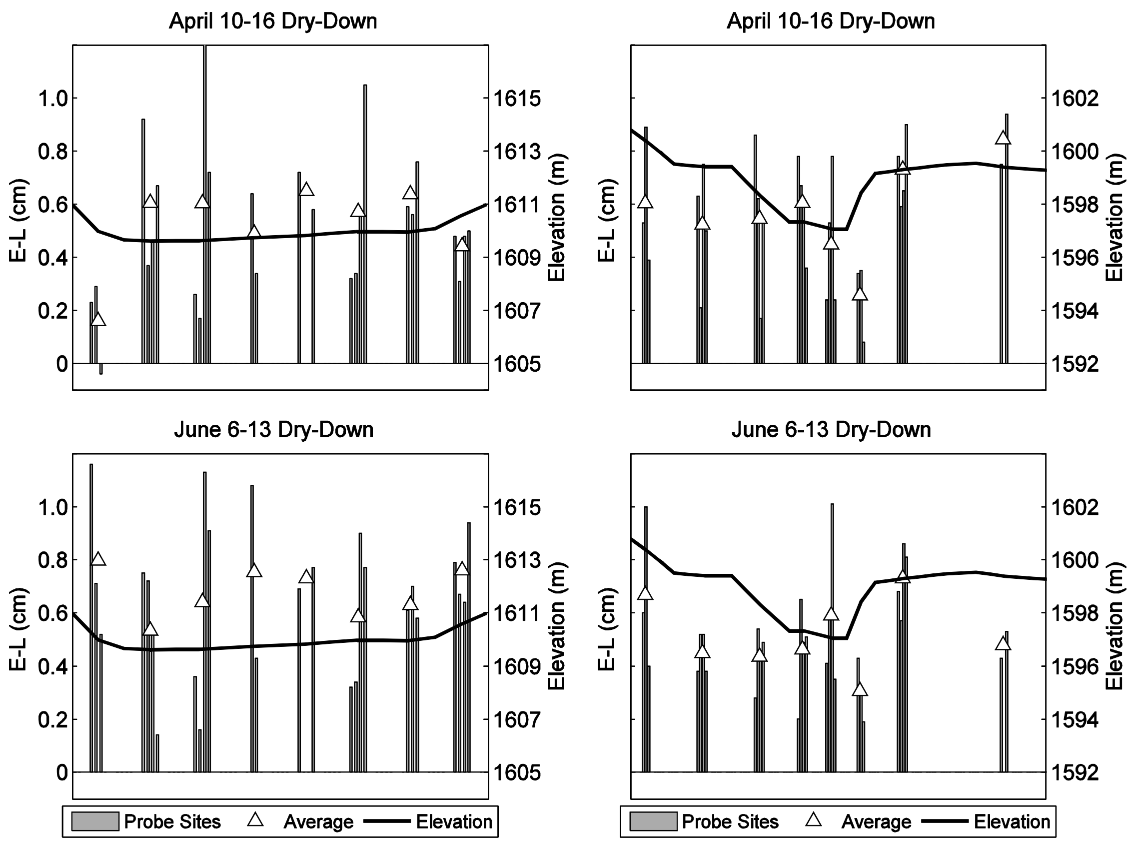

Figure 10. Plots of *E−L* for all probe locations with reliable data during the 6 day period following the 10 April and 5 June rainfall events across the ungullied and southwest gully sites (looking upstream). Black lines give a representative profile of the sites. Bars represent *E-L* for specific locations; triangles indicate the average of each topographic group. Positive values represent net evapotranspiration or lateral outflow; negative values represent net lateral inflow.

The prior analysis focused on the six day periods following two precipitation events. To gain a broader sense of the effects of gully topography on evapotranspiration rates and the associated dry-down in soil moisture, we look at the topography's impact on reference crop evapotranspiration (ET_0) during the entire eight month monitoring period. ET_0 is influenced by meteorological variables such as air temperature, relative humidity, wind speed, and solar radiation. Among these variables, gully topography is expected to most directly influence wind speed and solar insolation. As described in Section 2.2, wind speed was measured at the ungullied site, the upland between the two gullies, and the northeast gully bottom (locations shown in Fig 2). Wind speeds were similar at the ungullied site and the gully uplands. Figure 11a shows a plot of hourly wind speeds in the gully bottom and upland for each hour during the eight month observation time. Overall, wind speed in the gully bottom was on average 41% of that in the uplands, but the wind speed in the gully bottom is best fit with a regression line an intercept of -0.28 and thus a slope of 0.60. To assess the potential impacts of this difference on evapotranspiration, hourly ET_0 for a grass crop was computed for the monitoring period using measured values of temperature, relative humidity, and incoming shortwave solar radiation, as well as the wind speeds from the upland area and gully bottom using the Food and Agricultural Organization (FAO) Penman-Monteith equation (Allen et al., 1998). Fig. 11b shows the average ET_0 during each month of the observation period. The average ET_0 in the gully bottoms is 11.0% less than in the gully upland with the greatest percent difference occurring during the month of November (13.7%) and the greatest absolute difference in July (0.8 mm/day). This difference in ET_0 is expected to contribute to the greater dry-down rates seen in the uplands compared to gully bottoms (Fig. 6b).

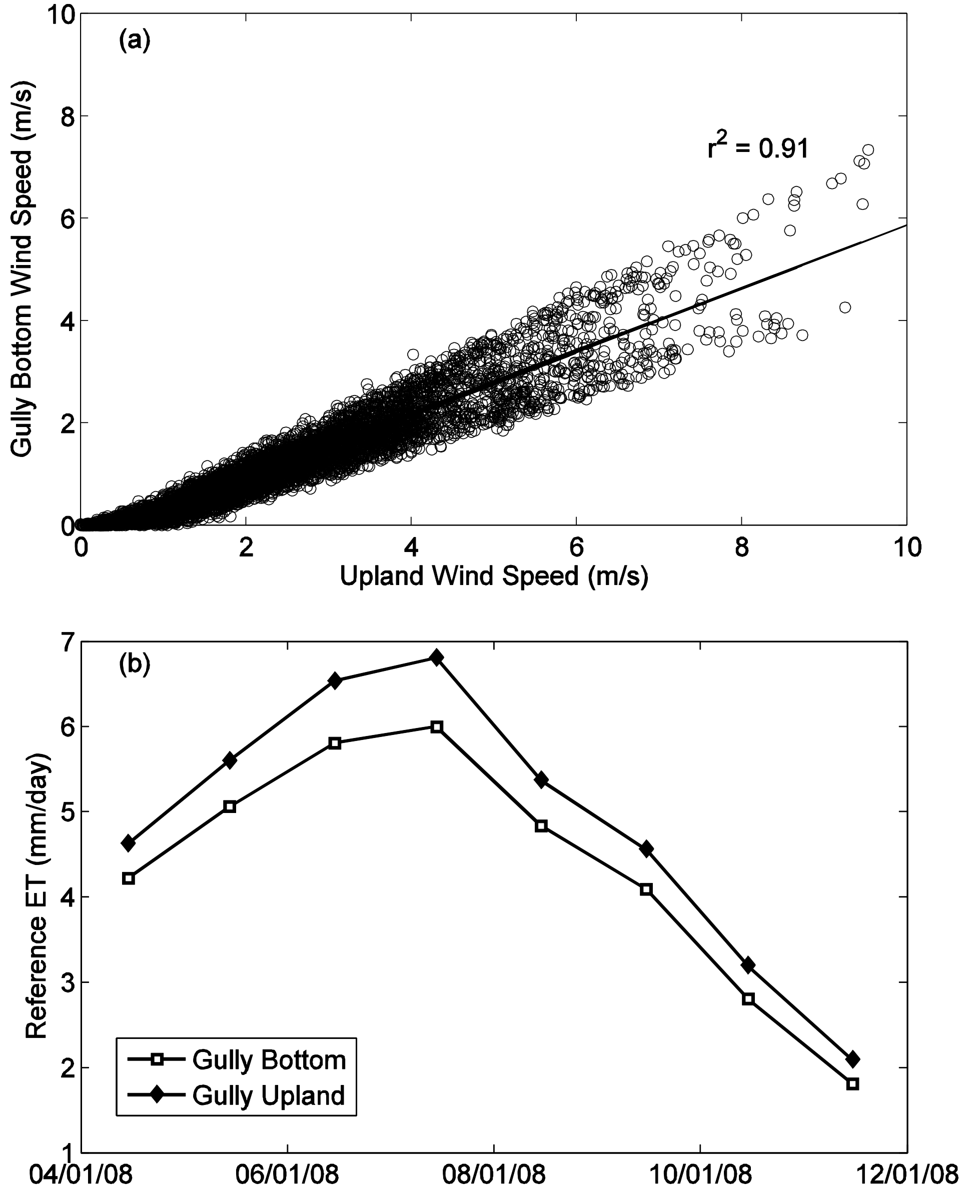

Figure 11. (a) Measured average hourly wind speed in the gully bottom plotted against measured average hourly wind speed in the gully upland during the entire monitoring period from April through November. The black line is a regression line that has a slope of 0.60 and intercepts the y-axis at -0.28. (b) Corresponding average monthly ET_0 using wind speeds from the gully bottom and gully upland. The other meteorological variables were assumed constant across the site and obtained from the gully upland meteorological station (except for air temperature and relative humidity, which were only measured at the ungullied site).

Another way that the gully topography might affect the evapotranspiration rates and thus soil moisture is through differences in solar insolation. The Penman-Monteith equation is typically applied using solar insolation on a horizontal surface, but the effects of the topographic slope and aspect can be incorporated using the potential solar radiation index (PSRI) (Moore et al., 1993). PSRI is defined as the ratio of the potential solar radiation on a sloping surface to that on a horizontal surface, and it depends on latitude, ordinal date, topographic slope, and aspect. PSRI, also called slope factor, was calculated for all permanent probe locations based on the method described by Dingman (2002) and the topographic survey described earlier. To assess the maximum impact of gully topography on insolation, average PSRI was calculated for the approximately south-facing (topographic group 6) and north-facing (topographic group 3) sidewalls of the southwest gully, which have the largest deviations from a flat location. Fig. 12a plots the average PSRI as a function of day of the year from April-November for the two sidewalls as well as the PSRI for a horizontal surface (which is always 1 by definition). During the observation period, PSRI varies from 0.7 to 2.3 on the south-facing sidewall and 0.1 to 0.9 on the north-facing sidewall. The largest deviations from 1 are observed at the end of the study period when the sun is low in the sky. Among the three cases, the south-facing sidewall receives the greatest insolation in the winter and the least insolation in the summer. Lee (1978) explains in detail why north-facing slopes can receive greater insolation in summer months. Fig. 12b shows the average monthly ET_0 as a function of time for the north and south-facing sidewalls and a flat surface. The only variable that differs in the calculation of ET_0 for the three cases is solar insolation. The average of gully bottom and upland wind speeds was used in all cases, and the remaining variables were obtained directly from the upland meteorological station (except for air temperature and relative humidity, which were only measured at the ungullied site). ET_0 on the north-facing slope is 82% less than on the south-facing slope in November but is 30% greater in June. The impact of these differences in solar insolation on soil moisture can be seen in Fig. 6c. Note that the north-facing sidewall experiences larger dry-downs than the south-facing sidewall during June and July when it has greater ET_0, but it has smaller dry-downs during October and November when it has lower ET_0.

An overall assessment of the effects of topographic-induced variations in wind speed and solar insolation on patterns of ET_0 from April-November was made at the ungullied and gully sites by estimating ET_0 at each probe location. Wind speed, PSRI, and other meteorological data were needed at each probe location to calculate ET_0. Hourly wind speed at the ungullied site was assumed to be spatially constant because the site has low relief. Hourly wind speed at the gully sites was estimated at each probe location by assuming that wind speed increased linearly with elevation between the gully bottom and upland. PSRI was calculated based on the local topographic slope and aspect as discussed previously. Measured values of air temperature and relative humidity were assumed to be spatially constant. At the ungullied site, estimated cumulative ET_0 for the study period was similar at all probe locations (slightly higher ET_0 on the south-facing valley side slope and slightly lower ET_0 on the north-facing valley side slope). At the gully sites, estimated cumulative ET_0 was greatest on the south-facing valley side slope (topographic group 13) and the upland areas (topographic groups 2, 7, and 8). Estimated cumulative ET_0 was least on the steep north-facing sidewalls (topographic groups 9 and 3).

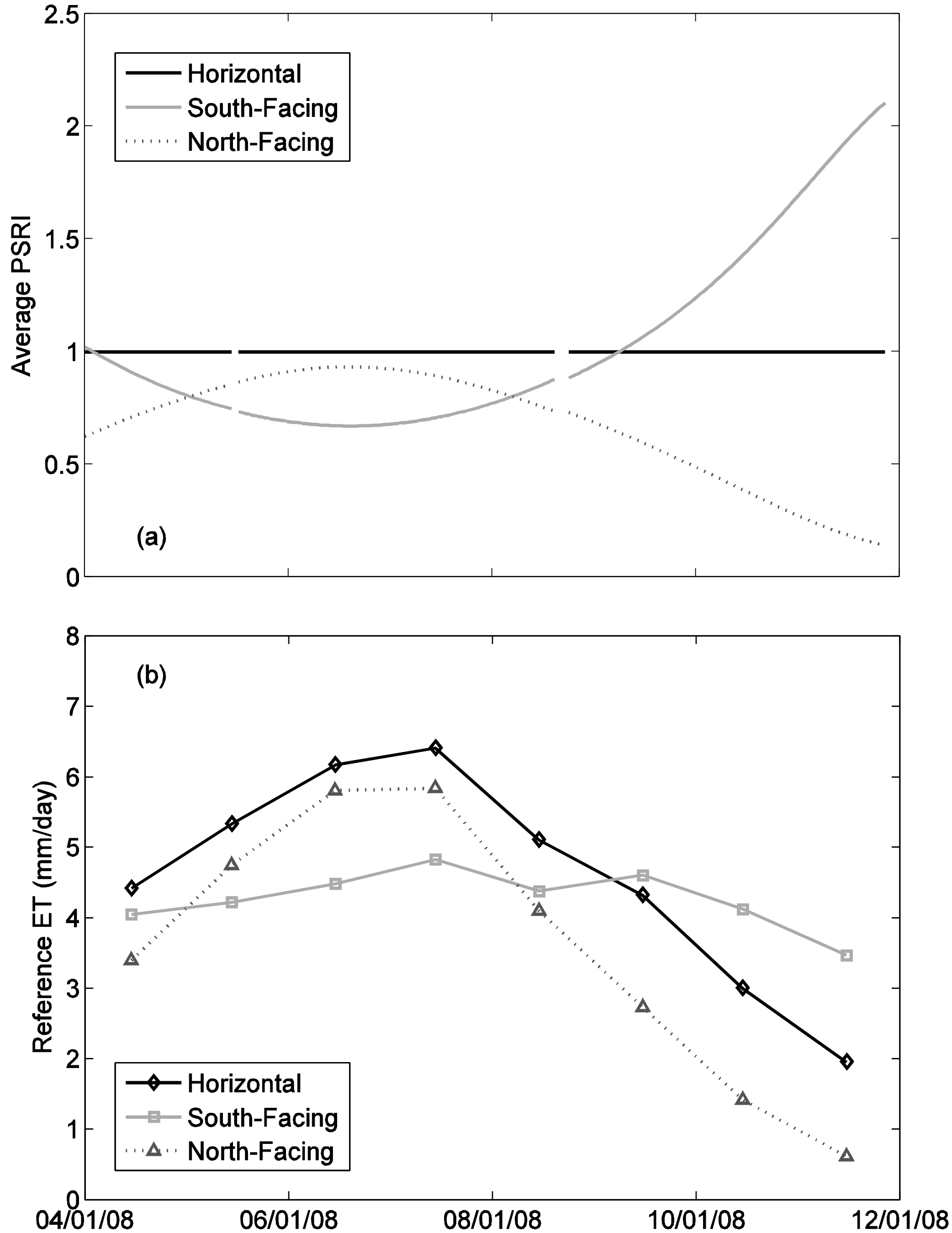

Figure 12. (a) Spatial average PSRI for the approximately south-facing sidewall (topographic group 6), north-facing sidewall (topographic group 3), and a horizontal surface as a function of day of the year for the monitoring period and (b) corresponding average monthly ET_0 during the observation period. ET_0 was calculated using PSRI values shown in (a), measured meteorological variables from the gully upland meteorological station (except for air temperature and relative humidity which were only measured at the ungullied site), and spatially constant wind speed (average of the upland and gully bottom wind speeds).

5. Conclusions

The primary conclusions of this paper are as follows:

1. Sand content tends to be lower in the gully bottoms than on the gully side slopes and uplands, but this tendency is quite weak. More variation in soil texture is observed between the two adjacent gully sites than within each gully site. These gullies are eroding through alluvial fills, which are expected to have their own patterns of texture variation. This result suggests that pre-existing soil texture variations in this case are more important than the soil texture variations associated with the modern gully topography.

2. When considering the time series of the site-wide average soil moisture, a larger difference is observed between the two gully sites with different soil textures than between the ungullied site and the northeast gully site, which have similar soil textures. This result suggests that the soil texture has a stronger impact on the spatial average soil moisture within these ~1500 m^2 sites than the presence of a gully does.

3. The occurrence of a gully in the study site was found to increase the spatial variability of the soil moisture immediately following precipitation events and during months with lower solar inclination. The increased variability after precipitation events occurs largely due to the rapid drying of the gully sidewall points and persistent wetness in the gully bottoms. The increased variability during months with lower solar inclination occurs because south-facing slopes dry more quickly than north-facing slopes.

4. Gully bottoms tend to be wetter and sidewalls tend to be drier than uplands and valley side slopes although significant variation is observed. During the months of August-November, average surface 10 cm soil moisture in the gully bottoms was 17.1% (0.026 m^3/m^3) greater than in the uplands and valley side slopes. This result contrasts with the work of van den Elsen et al. (2003), who found that soil moisture in uplands was slightly greater than soil moisture in the gully bottoms (measured soil moisture at depths of 15 cm and greater). Dense vegetation on the gully floor may reduce surface crusting and promote infiltration. In addition, although the reasons are not conclusive, portions of the gully bottoms appear to receive gradual lateral inflows for a period of 7-10 days after larger rainfall events. Gully sidewalls tend to be drier than the uplands due to rapid drainage during/after precipitation events and in some cases increased solar insolation.

5. Lower wind speeds are expected to contribute towards lower evapotranspiration rates in the gully bottoms. Measured wind speeds in the northeast gully bottom are on average 41% of the wind speeds in the uplands, which produces approximately an 11% reduction in the ET_0.

6. Temporal and spatial variation of solar insolation across the gullies is expected to contribute toward variability of ET_0, especially on north- and south-facing side slopes. ET_0 on the north-facing slope is 82% less than on the south-facing slope in November but is 30% greater in June.

Overall, this study considered how the presence of a gully impacts soil moisture variations in a semiarid grassland. It should be noted that, in general, gullies can have a wide range of morphologies including different widths, wall heights, etc. Furthermore, gullies can erode through a wide range of unconsolidated materials. Thus, a recommended line for future research is to examine the impacts that such morphological and substrate differences have on the results observed here.

References

Agassi, M., Shainberg, I., Morin, J., 1981. Effect of electrolyte concentration and soil sodicity on infiltration-rate and crust formation. Soil Science Society of America Journal, 45(5), 848-851.

Allen, R. G., Pereira, L. S., Raes, D., Smith, M., 1998. Crop evapotranspiration: guidelines for computing crop water requirements. FAO Irrigation and Drainage Paper, 56, 300 p.

Bradford, J. M., Piest, R. F., 1980. Erosional development of valley bottom gullies in the upper midwestern United States, in Thresholds in Geomorphology, edited by D. R. Coates and J. D. Vitek, 75– 101 pp., Allen and Unwin, St. Leonards, NSW, Australia.

Bromley, J., Brouwer, J., Barker, A. P., Gaze, S. R., Valentin, C., 1997. The role of surface water redistribution in an area of patterned vegetation in a semi-arid environment, south-west Niger. J. Hydrol., 198(1-4), 1-29.

Casenave, A., Valentin, C., 1992. A runoff capability classification-system based on surface-features criteria in semiarid areas of west Africa. J. Hydrol., 130(1-4), 231-249.

Collins, D. B. G., Bras, R. L., Tucker, G. E., 2004. Modeling the effects of vegetation-erosion coupling on landscape evolution. Journal Of Geophysical Research-Earth Surface, 109(F3).

Collins, D. B. G., Bras, R. L., 2007. Plant rooting strategies in water-limited ecosystems. Water Resources Research, 43(6).

Collins, D. B. G., Bras, R. L., 2008. Climatic control of sediment yield in dry lands following climate and land cover change. Water Resources Research, 44(10).

Dingman, S. L., 2002. Physical Hydrology, Second ed., 646 pp., Prentice Hall, Upper Saddle River.

Doe, W. W., Saghafian, B. 1992. Spatial and temporal effects of army maneuvers on watershed response: the integration of GRASS and a 2-D hydrologic model. 7th Annual GRASS Users Conference, Lakewood, CO.

Doe, W. W. I., Julien, P. Y., Ogden, F. L. 1997. Maneuversheds and watersheds: Modeling the hydrologic effects of mechanized training on military lands. Proceedings, 1997 American Water Resources Assoc. Summer Symposium, Keystone, CO.

Fitzjohn, C., Ternan, J. L., Williams, A. G., 1998. Soil moisture variability in a semi-arid gully catchment: implications for runoff and erosion control. Catena, 32(1), 55-70.

Fox, D. M., Bryan, R. B., Fox, C. A., 2004. Changes in pore characteristics with depth for structural crusts. Geoderma, 120(1-2), 109-120.

Gabris, G., Kertesz, A., Zambo, L., 2003. Land use change and gully formation over the last 200 years in a hilly catchment. Catena, 50(2-4), 151-164.

Gerakis, A., Baer, B., 1999. A computer program for soil textural classification. Soil Science Society of America Journal, 63(4), 807-808.

Gomez-Plaza, A., Martinez-Mena, M., Albaladejo, J., Castillo, V. M., 2001. Factors regulating spatial distribution of soil water content in small semiarid catchments. J. Hydrol., 253(1-4), 211-226.

Huo, Z., Shao, M. A., Horton, R., 2008. Impact of gully on soil moisture of shrubland in wind-water erosion crisscross region of the Loess Plateau. Pedosphere, 18(5), 674-680.

Idso, S. B., Jackson, R. D., Reginato, R. J., Kimball, B. A., Nakayama, F. S., 1975. Dependence of bare soil albedo on soil-water content. Journal of Applied Meteorology, 14(1), 109-113.

Istanbulluoglu, E., Bras, R. L., Flores-Cervantes, H., Tucker, G. E., 2005. Implications of bank failures and fluvial erosion for gully development: Field observations and modeling. Journal Of Geophysical Research-Earth Surface, 110(F1).

Jackson, T. J., Schmugge, T. J., 1989. Passive microwave remote-sensing system for soil-moisture - some supporting research. IEEE Trans. Geosci. Remote Sensing, 27(2), 225-235.

Kerr, Y. H., 2007. Soil moisture from space: Where are we? Hydrogeology Journal, 15(1), 117-120.

Lee, R., 1978. Forest Microclimatology, 171-173 pp., Columbia Univ. Press, New York.

Mills, A. J., Fey, M. V., 2004. Frequent fires intensify soil crusting: physicochemical feedback in the pedoderm of long-term burn experiments in South Africa. Geoderma, 121(1-2), 45-64.

Moore, I. D., Burch, G. J., Mackenzie, D. H., 1988. Topographic effects on the distribution of surface soil-water and the location of ephemeral gullies. Trans. ASAE, 31(4), 1098-1107.

Moore, I. D., Norton, T. W., Williams, J. E., 1993. Modeling environmental heterogeneity in forested landscapes. J. Hydrol., 150(2-4), 717-747.

Morin, J., Benyamini, Y., 1977. Rainfall infiltration into bare soils. Water Resources Research, 13(5), 813-817.

Njoku, E. G., Entekhabi, D., 1996. Passive microwave remote sensing of soil moisture. J. Hydrol., 184(1-2), 101-129.

Nolan, M., Fatland, D. R., Hinzman, L., 2003. DInSAR measurement of soil moisture. IEEE Trans. Geosci. Remote Sensing, 41(12), 2802-2813.

Patton, P. C., Schumm, S. A., 1981. Ephemeral-stream processes: Implications for studies of quaternary valley fills. Quat. Res., 15(1), 24-43.

Poesen, J., 1986. Surface sealing as influenced by slope angle and position of simulated stones in the top layer of loose sediments. Earth Surface Processes and Landforms, 11(1), 1-10.

Rodriguez-Iturbe, I., D'Odorico, P., Porporato, A., Ridolfi, L., 1999. On the spatial and temporal links between vegetation, climate, and soil moisture. Water Resources Research, 35(12), 3709-3722.

Schmugge, T. J., 1983. Remote-sensing of soil-moisture - recent advances. IEEE Trans. Geosci. Remote Sensing, 21(3), 336-344.

Schumm, S. A., Harvey, M. D., Watson, C. C., 1984. Incised Channels: Morphology, Dynamics and Control, 200 pp., Water Resour. Publ., Highlands Ranch, Colo.

Shainberg, I., Singer, M. J., 1985. Effect of electrolytic concentration on the hydraulic-properties of depositional crust. Soil Science Society of America Journal, 49(5), 1260-1263.

Shaw, R. B., Anderson, S. L., Schulz, K. A., Diersing, V. E., 1989. Plant communities, ecological checklist, and species list for the U.S. Army Pinon Canyon Maneuver Site, Colorado, Colorado State University Department of Range Science, Science Series No. 37, 71 p.

Stevens, M. R., Dupree, J. A., Kuzmiak, J. M., 2008. Temporal and spatial variations in precipitation, streamflow, suspended-sediment loads and yields, and land-condition trend analysis at the U.S. Army Piñon Canyon Maneuver Site, Las Animas County, Colorado, 1983 through 2007: U.S. Geological Survey Scientific Investigations Report 2008–5111, 47 p.

Teuling, A. J., Troch, P. A., 2005. Improved understanding of soil moisture variability dynamics. Geophysical Research Letters, 32(5).

Topp, G. C., Davis, J. L., Annan, A. P., 1980. Electromagnetic determination of soil-water content measurements in coaxial transmission lines. Water Resources Research, 16(3), 574-582.

Trout, T. J., Johnson, L. F., Gartung, J. 2008. Remote sensing of canopy cover in horticultural crops.

Tucker, G. E., Arnold, L., Bras, R. L., Flores, H., Istanbulluoglu, E., Solyom, P., 2006. Headwater channel dynamics in semiarid rangelands, Colorado high plains, USA. Geological Society of America Bulletin, 118(7-8), 959-974.

U.S. Soil Conservation Service, 1983. Soils manuscript for the Pinon Canyon Maneuver Site: Trinidad, Colo., U.S. Department of Agriculture, unpublished, 157 p.

U.S. Army Corps of Engineers, 1999. Biological soil crusts for arid land rehabilitation, Construction Engineering Research Laboratory, Fact Sheet, 2 p.

Valentin, C., Poesen, J., Li, Y. 2005. Gully erosion: Impacts, factors and control, Elsevier Science Bv.

van den Elsen, E., Xie, Y., Liu, B. Y., Stolte, J., Wu, Y. Q., Trouwborst, K., Ritsema, C. J., 2003. Intensive water content and discharge measurement system in a hillslope gully in China. Catena, 54(1-2), 93-115.

von Guerard, P., Abbot, P. O., Nickless, R. C., 1987. Hydrology of the US Army Pinon Canyon maneuver site, Las Animas County, Colorado: Denver, Colorado, Water-Resources Investigations Report 87-4227, U.S. Department of the Interior.

Wigneron, J. P., Calvet, J. C., Pellarin, T., Van de Griend, A. A., Berger, M., Ferrazzoli, P., 2003. Retrieving near-surface soil moisture from microwave radiometric observations: current status and future plans. Remote Sensing of Environment, 85(4), 489-506.

Zheng, J. Y., Wang, L. M., Shao, M. A., Wang, Q. J., Li, S. Q., 2006. Gully impact on soil moisture in the gully bank. Pedosphere, 16(3), 339-344.